CONTAINMENT OF SINGLE-SPECIES PLASMAS AT LOW ENERGIES

C. F. Driscoll

Department of Physics
University of California, San Diego
La Jolla, CA 92093

For some purposes, it may be convenient to store or transport anti-protons in cylindrical traps rather than in storage rings. This talk will describe some of the theoretical perspectives and experimental results developed in the UCSD program on containment of pure electron plasmas. My remarks will fall into 5 general areas:

(1) Practical limits on magnetic fields and containment voltages limit the number of charges stored, with 10^{13} being moderately difficult.

(2) Long-term containment of the particles depends on cylindrical symmetry and conservation of the total angular momentum of the plasma, so small asymmetries can cause significant losses.

(3) The Newton-Maxwell equations almost scale with respect to charge and mass, so much of the physics of pure electron plasmas applies to pure ion plasmas.

(4) The detection and transmission of azimuthally asymmetric plasma waves may be important for diagnostics and for dynamical stabilization of the plasma.

(5) Confined thermal equilibrium states exist for unneutralized plasmas at high or low temperatures, even for more than one charge species.

Cylindrical Containment.

A simplified diagram of a cylindrical electron plasma containment apparatus is shown in Figure 1a. The entire apparatus is in a uniform magnetic field B_z, and evacuated to below 10^{-10} Torr. The system is repetitively pulsed in the following sequence. Initially cylinders A and B are grounded, and cylinder C is biased strongly negative. Electrons emitted from a negatively biased thermionic source[1,2] then form a column from the source through cylinder B. When cylinder A is biased negative, the electrons are axially trapped by the electrostatic fields. The unneutralized space charge generates a strong radial electric field, and some radial transport may occur with time.[3,4]
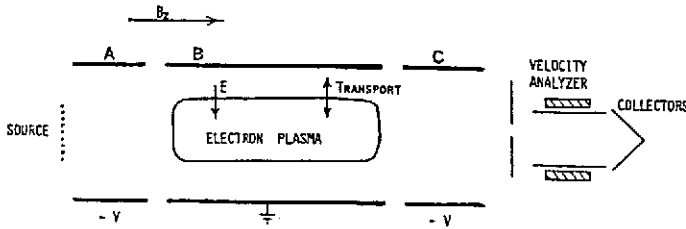
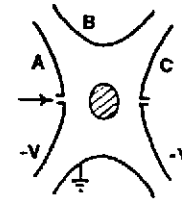Figure 1a. The cylindrical containment geometry.

Figure 1b. Hyperbolic electrodes for a Penning trap.

After a containment time t, cylinder C is pulsed to ground potential, and the electrons stream along field lines to collimators, velocity analyzers, and collectors. Repetition of the cycle many times with different containment times and different collection radii allows us to construct the density and temperature evolutions $n(r,t)$ and $T(r,t)$. The group at UCSD currently operates two types of electron plasma apparatuses: a room-temperature devices with parameters $n \sim 10^7$ cm^{-3}, $kT \sim 1$ eV, $R_p \sim 1$ cm, $L_p \lesssim 100$ cm, $B \lesssim 100$ G, $P \lesssim 10^{-10}$ Torr; and a cryogenic apparatus with $n \sim 10^{10}$ cm^{-3}, $kT \gtrsim 10^{-3}$ eV, $L_p > R_p \sim 0.1$ cm, $B \lesssim 50$ kG, $P < 10^{-12}$ Torr.

Groups interested in atomic physics often contain elementary particles or ions in "Penning" traps with electrodes in the shape of hyperboloids of revolution,[5-8] as in Figure 1b. Here, the axial containment is provided by end caps A and C, which have holes for particle injection or removal. Functionally, the two designs are very similar, each having some advantages and disadvantages. The purpose of the hyperbolic electrodes is to create cylindrically symmetric potentials of the form $\Phi = A(r^2-2z^2) + \Phi_0$ over the entire containment volume, so that a trapped particle will move in an analytically simple potential. The cylindrical electrodes of Figure 1 necessarily give this same potential profile near $r=z=0$, but the functional form becomes more complicated near the electrodes.

When enough particles are contained so as to form a plasma, however, the axial electric field is shielded inside the plasma.[9] The individual particle dynamics are then dominated by the collective effects of shielding and wave modes, with the details of the electrostatic boundaries of less importance. This transition can be expected to occur when the Debye shielding distance becomes less than the size of the plasma. Since

$$\lambda_D \equiv (kT/4\pi e^2 n)^{1/2} = 0.74 \, T_{eV}^{1/2} (n/10^6)^{-1/2} \quad \text{(cm)} \quad , \qquad (1)$$

centimeter-sized collections of particles in the $1-10^2$ eV range can be expected to exhibit collective effects at densities $n \sim 10^6 - 10^8$ cm^{-3}.

Space charge potential determines one of the two fundamental limits to the number of unneutralized charges that can be contained in any trap. Consider a long, uniform column of N_T total electrons with radius R_p and length L inside a grounded cylinder of radius R_w, as in Figure 1a. Poisson's equation then gives the space charge potential at $r = 0$ in the plasma as

$$\Phi_0 = -1.4 \times 10^{-7} \frac{N_T}{L} (1 + 2 \ln \frac{R_w}{R_p}) \quad \text{(Volts)} . \qquad (2)$$

For axial containment, electrodes A and C must be more negative than Φ_0 by several kT/e. A 100 cm-long trap with $R_w = 1.5 R_p$ would thus require voltages greater than 25 kV to contain $N_T = 10^{13}$ electrons. Here, one advantage of the elongated cylindrical geometry becomes apparent: the required containment voltages are inversely proportional to L. For a nearly spherical plasma, as is often obtained with hyperbolic electrodes, a similar formula is obtained with the plasma diameter setting the scale instead of L; furthermore, only 1/2 of the containment voltage V is effective, since the Laplace potential Φ_0 at $r = z = 0$ is $V/2$ before any particles are added. From the perspective of Eqn. (2), the recent suggestion[10] that a milligram (6×10^{20}) of unneutralized anti-protons can be trapped seems somewhat optimistic.

Macroscopic radial force balance determines the second fundamental containment limit for unneutralized plasmas, called the Brillouin limit. Consider a uniform, cold electron fluid rotating with $v_\theta = \omega r$. Then, the balance between the Lorentz force and centrifugal force requires

$$-neE - ne \frac{\omega r}{c} B + nm \omega^2 r = 0 . \qquad (3)$$

Taking $E = -2\pi enr$, and defining $\omega_p^2 = 4\pi e^2 n / m$ and $\Omega = eB/mc$, a solution for ω exists only if

$$\omega_p^2 < \Omega^2/2 . \qquad (4)$$

This gives a density limit for protons of

$$n_p \lesssim 2.6 \times 10^9 (B/10 \text{ kG})^2 \quad (\text{cm}^{-3}) . \qquad (5)$$

Again, a rather severe constraint exists: even in a field of 100 kG, the maximum proton density attainable is 2.6×10^{11} cm^{-3}.

Interestingly, Eqn. (4) can be re-written as $nmc^2 \lesssim B^2/8\pi$: the rest energy of the particles contained will be less than the magnetic field energy in the same volume. For perspective, this compares rather unfavorably with a similar limit for the containment of *neutralized* plasmas, given by $nkT \lesssim B^2/8\pi$. When the unneutralized plasma has a finite temperature, the gradient of the pressure will give an additional outward force in Eq. (3).

This will reduce the maximum particle density which can be contained in a given B field. However, this effect is significant only for temperatures high enough that $\lambda_D \gtrsim R_p$.

The cylindrical containment geometry of Figure 1a makes possible a number of useful techniques for axial manipulation of the plasma. A typical apparatus might have 10 containment cylinders, rather than the 3 shown in Figure 1, and the plasma can then be axially compressed or expanded by changing the voltages on the various electrodes. It is possible, for example, to accumulate particles at low density in one region, then repetitively "stack" these particles into a higher density region. Of course, there will also be heating or cooling of the parallel thermal energies associated with axial compression or expansion. For example, during repetitive stacking, careful matching of the various potentials is required so as not to pump the particles to high energies. Particles with sufficiently high energy will "evaporate" over the containment potentials; conceivably, this evaporation could be used to separate the particles by energy for cooling purposes.

Loss Processes.

Unneutralized plasmas in cylindrical geometry are unique in that they can, in theory, be confined forever.[11] In experiments, however, there are always loss processes, and containment times in the range of $1-10^6$ seconds are typically obtained.[3,4,12-14]

The magnetic containment of an unneutralized plasma is most readily understood in terms of the total canonical angular momentum, given by[9,11]

$$ P_\theta = \sum_j \left[mv_{\theta j} r_j + \frac{q_j}{c} A_\theta(r_j) r_j \right] , \tag{6} $$

where $A_\theta(r) = Br/2$. The limit of large field is particularly simple, in that the mechanical part of the angular momentum is negligible. For a single charge species we may then write

$$ P_\theta \approx \frac{qB}{2c} \sum_j r_j^2. $$

To the extent that P_θ is conserved, the mean square radius of the plasma cannot change. (In contrast, if there were both positive and negative charges, an oppositely charged pair could move across the field without changing P_θ.)

All like-particle interactions within the plasma conserve P_θ, and cannot lead to plasma expansion and loss. Thus, there is no analogy to the losses from "intra-beam scattering" in toroidal beam systems. Rather, these internal interactions cause transport towards a confined, global thermal equilibrium state as will be discussed below.
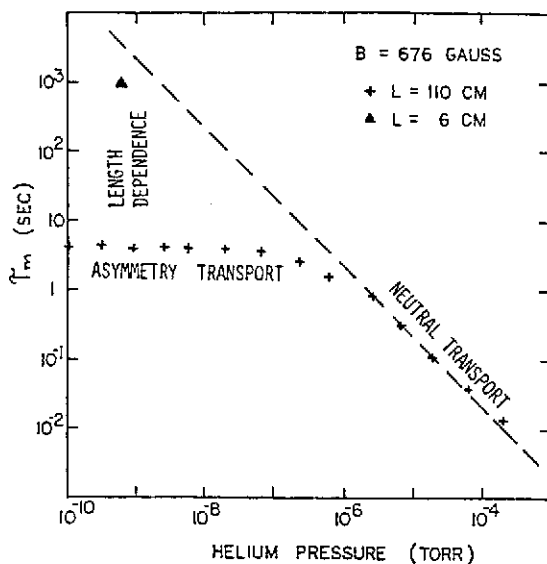
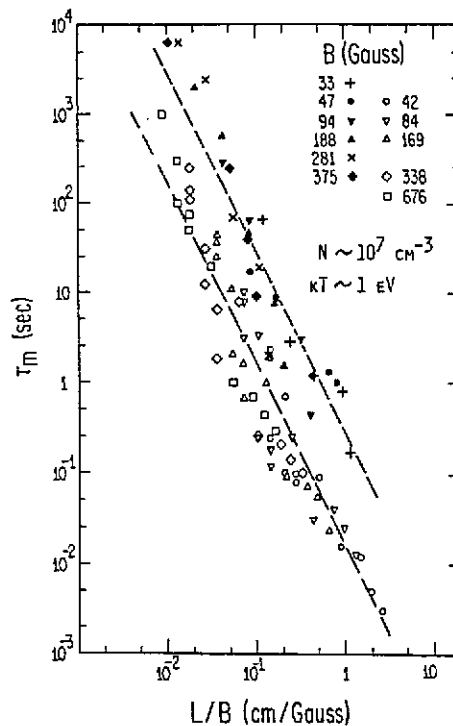Figure 2. Containment times as a function of neutral pressure.

Figure 3. Measured containment times τ_m versus plasma length L divided by magnetic field B, for two apparatuses.

The plasma can expand only if azimuthally asymmetric forces from outside the plasma act on the particles. Experimentally, one always observes a radial spreading of the plasma on some time scale. To characterize these loss processes, we measure the time τ_m required for the central density to decrease a factor of two, due to radial expansion by $\approx\sqrt{2}$. The time τ_m thus characterizes the time required for these external torques to decrease the angular momentum of the plasma by about a factor of two.

In Figure 2, we plot the experimentally measured containment time τ_m versus neutral background pressure P.[4] At high pressures, we find $\tau_m \propto P^{-1}$, as expected: the stationary neutrals exert a drag on the rotating electron column, decreasing P_θ and allowing expansion.[4,15] However, as the pressure is decreased below 10^{-7} Torr, τ_m ceases to increase. We believe that this loss at low pressures is due to electrostatic or magnetostatic asymmetries in the containment apparatus.

A striking feature of this asymmetry-induced transport is that it is a strong function of the length L of the contained plasma.[12,14] As shown in Figure 2, when the length is decreased from 110 cm to 6 cm, τ_m increases from 4 sec to 1000 sec. This length-dependent loss is observed over the entire accessible range of lengths and magnetic fields on two room-

temperature electron containment apparatuses, as shown in Figure 3. For each apparatus, the containment times scale approximately as $(L/B)^{-2}$ over 5 decades, with about a decade of (reproducible) scatter. The newer of the two apparatuses was built with particular attention to minimization of construction asymmetries in the electric and magnetic field structures, and the resulting containment times improved a factor of 20.

We do not yet understand the mechanism by which asymmetries couple angular momentum into the plasma,[16] but these losses do appear to be generic to nonneutral plasma containment in cylindrical geometry. We also do not know how this loss process scales with n or kT, although it is likely that the loss rate increases at least linearly with density. This suggests that if long plasma columns at high densities are required to contain a sufficient number of particles, then active containment enhancement techniques (as discussed below) may be required.

CFD 2021: This size scaling is questionable, as it does not preserve e^2/mc^2, which is a fundamental constant.

Electron-Proton Scaling

Much of the physics of pure electron plasmas applies equally well to proton or ion plasmas, with a simple scaling between the two. In particular, Newton's equation of motion and Maxwell's equations can be scaled with respect to mass and charge, except for the Maxwell's $\nabla \times b$ equation. Specifically, consider the Newton-Maxwell equations for the positions $\tilde{r}_j(t)$ and fields $\tilde{e}(\tilde{r},t)$ and $\tilde{b}(\tilde{r},t)$ associated with electrons of mass m and charge q. These equations can be re-scaled for the positions $\tilde{R}_j(T)$ and fields $\tilde{E}(\tilde{R},T)$ and $\tilde{B}(\tilde{R},T)$ associated with ions of mass $M = \mu m$, charge $Q = \chi q$, by defining

$$T = \tau t \qquad\qquad \tau = \mu^{1/2}|\chi|^{-1}\rho^{3/2}$$
$$\tilde{E} = \epsilon \tilde{e} \qquad \text{with} \qquad \epsilon = \chi \rho^{-2}$$
$$\tilde{B} = \beta \tilde{b} \qquad\qquad \beta = \mu^{1/2}\chi|\chi|^{-1}\rho^{-3/2} \qquad (8)$$
$$\tilde{R} = \rho \tilde{r} \qquad\qquad \rho = \text{arbitrary}$$

The re-scaled equations are then

$$M\frac{d^2\tilde{R}_j}{dT^2} = Q\left[\tilde{E} + \frac{1}{c}\frac{d\tilde{R}_j}{dT} \times \tilde{B}\right]$$

$$\nabla \cdot \tilde{E} = 4\pi Q \sum_j \delta(\tilde{R}-\tilde{R}_j)$$

$$\nabla \times \tilde{E} = -\frac{1}{c}\frac{\partial}{\partial t}\tilde{B} \quad , \quad \nabla \cdot \hat{B} = 0 \qquad (9)$$

$$\nabla \times \tilde{B} = \left\{\mu\chi^{-2}\rho\right\}\left[\frac{4\pi}{c} Q \sum_j \frac{d\tilde{R}_j}{dT}\delta(\tilde{R}-\tilde{R}_j) + \frac{1}{c}\frac{\partial \tilde{E}}{\partial T}\right] .$$

These are again the Newton-Maxwell equations, except for the $\nabla \times B$ equation which is in error by the factor $\mu\chi^{-2}$. Thus, for those ion plasma effects

which are electrostatic in nature, electron plasma experiments will give analogous results.

For $\rho=1$, the scaling requires that the magnetic field for ions is larger by $(M/m)^{1/2}$, that the containment voltages are larger by the charge ratio χ, and that the initial kinetic energies of the ions are larger by χ^2. The ion dynamics will then be the same as the electron dynamics, except that the ions will evolve slower by a factor of $(M/m~\chi^2)^{1/2}$. For example, consider containing protons in an apparatus similar to that giving the solid data points of Figure 3, with parameters $n_p = 10^7$, $kT = 1$ eV, $B = 4.3$ kG, $L = 100$ cm. The analogous electron experiment with $B = 100$ G, $L = 100$ cm gives $\tau_m = 0.3$ sec, suggesting that protons would have a containment time of about 13 seconds.

Of course, the electron and ion systems are not identical. The $\nabla \times b$ Maxwell equation must be included to describe cyclotron radiation, which can be an important cooling mechanism for electrons at high fields,[17] but not for ions. The most important difference between the electron and ion plasmas results from effects outside the scope of the Newton-Maxwell equations. For example, the collision of an ion with another object must be described by quantum mechanics, and is thus not subject to the above scaling. Indeed, whereas neutral collisions generally cause angular momentum loss and resultant heating of electron plasmas,[4,15] these collisions may result in substantial cooling of ion plasmas.[5,6,8]

Azimuthally Asymmetric Waves.

When an unneutralized plasma becomes sufficiently dense that $\lambda_D < R_p$, collective modes of the form $A(r)\exp[ikz + il\theta - i\omega t]$ become important. Understanding losses may require diagnostics of these modes, and dynamical control of the plasma may require transmitters coupling to the plasma modes. In general, an unneutralized plasma will exhibit a variety of modes almost as complex as found in neutral plasmas.[9]

These charge density fluctuations are readily detected by measuring the image charge fluctuations in particular azimuthal sections of the cylindrical wall, as shown in Figure 4. A complete 360° cylinder will detect only $l = 0$ modes, 180° sections will detect modes with $l = 1,3,5...$, appropriately connected 90° sections will detect $l = 2,4,6...$, etc. By taking separate frequency spectra with different antenna configurations, the azimuthal mode numbers of the various spectral components can be identified.
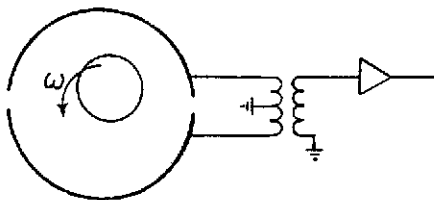

Figure 4. Receiver to detect the ℓ=1 diocotron mode.

It should be noted that the voltages induced on the wall sectors are themselves asymmetries which can couple back into the plasma. For example, when a 1 kΩ resistance is connected between wall sectors on electron containment devices, the $l=1$, $k=0$ diocotron mode is observed to grow exponentially on a time scale of 0.1 seconds.[18] (Without the wall resistances, the mode is neutrally stable.) This mode corresponds to a uniform shift of the plasma column off center, with the off-center column rotating about the center of the containment cylinder, as depicted in Figure 4. Of course, this mode may be driven unstable by any other resistances to the azimuthal flow of image currents, such as finite wall conductivity.

Interestingly, the $l=1$ diocotron mode can be made to damp to zero by replacing the wall resistances with feedback amplifiers.[18] If the wave is received on one set of wall probes and then applied to another set 180° out of phase, the off-center plasma column can be moved back on center. In this way, pure electron columns can be moved substantially off-center, then moved back, with no significant spreading of the column.

Launched waves can also cause the diameter of a centered plasma column to decrease.[16] The launched waves should propagate in the $\hat{\theta}$ direction *faster* than the plasma column is rotating. Then absorption of the wave by the plasma will increase the angular momentum of the plasma, causing $<r^2>$ to decrease. (This is essentially the opposite of the effect of collisions with stationary neutral atoms.) Of course, phased launching techniques must be used so that the complementary mode travelling in the $-\hat{\theta}$ direction will not also be launched. These techniques may be thought of as analogous to the stabilization and cooling of storage rings with kickers.

Equilibrium States.

Like-particle interactions cause internal transport of energy and particles, and cause the unneutralized plasma to relax to a confined global thermal equilibrium state.[19,20] For a single charge species, the equilibrium distribution is

$$f\left(\tilde{r},\tilde{v}\right) = \tilde{n}\left(\tilde{r}\right) \exp\left[-\frac{m}{2kT}(\tilde{v}-\omega r\hat{\theta})^2\right]. \tag{10}$$

This is just a Maxwellian velocity distribution rotating as a rigid rotor. The density profile $n\left(\tilde{r}\right)$ is essentially constant out to some surface of revolution, and then falls exponentially to zero in a few Debye lengths. It should be emphasized that this equilibrium state is just as accessible and stable at finite temperatures as at cryogenic temperatures.

The time scale to approach equilibrium depends on the dominant like-particle interaction mechanism. Like particle collisions result in velocity scatterings which give equilibration on a time scale $[\nu(r_L/\lambda_D)^4]^{-1}$, where ν is the 90° scattering time, and the Larmor radius $r_L \equiv \bar{v}/\Omega$.[19] Other

longer-range interactions giving faster equilibration on a time scale $[\nu(r_L/\lambda_D)^2]^{-1}$ have been predicted[21] and observed.[22] This particle transport is due to viscous forces arising from shears in the rotation velocity of non-equilibrium density profiles. Equilibration times for a proton plasma with $n_p = 10^7$, $kT = 1$ eV, $B = 4.3$ kG would probably be on the order of 10 sec. This time would be expected to decrease as n increases or kT decreases. Of course, the containment system must be sufficiently symmetric that loss processes are small on the time scale for equilibration.

For an isolated system, the initial total number of particles, angular momentum, and energy of the plasma determine the three equilibrium parameters of R_p/λ_D, ω, and kT.[19] However, the equilibrium parameters can be manipulated experimentally by any coupling which causes the total energy or total angular momentum of the system to change.

For example, ion plasmas have been cooled to temperatures of a few degrees Kelvin or less using several different techniques. Ion-neutral collisions can cause ion cooling, depending on the neutral energy absorption and momentum transfer cross-sections. Barlow et al[8] report ion plasmas cooling to an estimated 13° K after the ionizing beam is turned off. In this system, selective "evaporation" of the more energetic ions also contributes to ion cooling. Surko et al[23] are presently constructing an apparatus to contain and cool a positron plasma, using inelastic positron-neutral collisions.

More esoterically, tuned laser-ion interactions can be used to cool the ions as well as to maintain a small radial profile. Bollinger and Wineland[6,7] report cooling of small collections of 10^2–10^3 ions to temperatures of order 0.1° K. In this system, the laser is tuned to near an atomic transition, and the absorbed momentum of the photon both moves high thermal energy electrons to lower energies, and globally changes the total plasma momentum so as to decrease the mean radius. (This latter effect is similar to the effect of the azimuthally propagating launched waves discussed above.)

In any discussion of plasma cooling, it must be kept firmly in mind that any radial expansion of the plasma (due to external torques) will probably cause significant heating. As the plasma expands, the large electrostatic energy of the space charge field can be converted to thermal energy through Joule heating. In the time τ_m required for the plasma to expand a factor of $\sqrt{2}$ in radius, approximately 1/2 of the space charge energy will be converted.

For example, a cryogenic electron plasma apparatus at UCSD contains electrons with parameters $n \sim 10^{10}$ cm^{-3}, $B \sim 50$ kG, with a central space charge potential $\Phi_0 \sim 1$ kV. The heating power due to expansion can be approximated as $e\,\Phi_0/\tau_m$. The electrons cool due to cyclotron radiation, with a cooling power $P_c = kT/\tau_c$, where $\tau_c \simeq 0.15$ sec. Equating the heating and cooling powers gives an equilibrium temperature

$$kT_{eq} \sim \frac{\tau_c}{\tau_m} e \, \Phi_0 \; . \tag{10}$$

Thus, containment times $\tau_m \sim 10^5$ sec are required (and obtained in practice) to obtain $kT_{eq} \sim 10^{-3}$ eV.[13]

It has been suggested that cyclotron radiation from a small number of electrons can be used to cool a cloud of anti-protons.[24] Here, the same considerations as above apply, except that the effecting cooling power is decreased because there is less than one electron per anti-proton. A second, more subtle, consideration is that the electrons and anti-protons would tend to separate spatially: the thermal equilibrium state for would exhibit centrifugal separation, with the electrons in the center and the anti-protons to the outside.[25] The amount of spatial overlap of the two species would decrease as the temperature decreased or as the densities increased. These separated equilibria have been studied theoretically, but not yet observed, and a number of processes could contribute to the heat and particle transport as the equilibrium state is approached.

These and other considerations suggest that while it may indeed be practical to store moderate numbers of unneutralized anti-protons at low energies, there will be a number of interesting plasma physics problems to be dealt with in the process.

Acknowledgments

References

1. J. H. Malmberg and J. S. deGrassie, "Properties of a Nonneutral Plasma," Phys. Rev. Lett. **35**, 577 (1975).

2. C. F. Driscoll and J. H. Malmberg, "Hollow Electron Column from an Equipotential Cathode," Phys. Fluids **19**, 760 (1976).

3. J. S. deGrassie and J. H. Malmberg, "Wave-Induced Transport in the Pure Electron Plasma," Phys. Rev. Lett. **39**, 1077 (1977); J. S. deGrassie and J. H. Malmberg, "Waves and Transport in the Pure Electron Plasma," Phys. Fluids **23**, 63 (1980).

4. J. H. Malmberg and C. F. Driscoll, "Long-Time Containment of a Pure Electron Plasma," Phys. Rev. Lett. **44**, 654 (1980).

5. H. G. Dehmelt in *Atomic Physics*, D. Kleppner and F. M. Pipkin, eds. (Plenum, 1981), vol. 7, p. 337.

6. J. J. Bollinger and D. J. Wineland, "Strongly Coupled Nonneutral Ion Plasma," Phys. Rev. Lett. **53**, 348 (1984).

7. D. J. Wineland and W. M. Itano, "Laser Cooling of Atoms," Phys. Rev. **A20**, 1521 (1979).

8. S. E. Barlow, G. H. Dunn, and M. Schauer, "Radiative Association of CH_3^+ and H_2 at 13 K," Phys. Rev. Lett. **52**, 102 (1984).

9. R. C. Davidson, *Theory of Nonneutral Plasmas* (Benjamin, 1974).

10. R. L. Forward, "Antiproton Annihilation Propulsion," AFRPL-TR-85-034, Edwards AFB (1985).

11. T. M. O'Neil, "Nonneutral Plasmas Have Exceptional Confinement Properties," Comments Plasma Phys. Cont. Fusion **5**, 231 (1980); T. M. O'Neil, "A Confinement Theorem for Nonneutral Plasmas," Phys. Fluids **23**, 2216 (1980).

12. C. F. Driscoll and J. H. Malmberg, "Length-Dependent Containment of a Pure Electron Plasma," Phys. Rev. Lett. **50**, 167 (1983).

13. J. H. Malmberg and T. M. O'Neil, "The Pure Electron Plasma, Liquid and Crystal," Phys. Rev. Lett. **39**, 1333 (1977); J. H. Malmberg, T. M. O'Neil, A. W. Hyatt and C. F. Driscoll, "The Cryogenic Pure Electron Plasmas," Proceedings of 1984 Sendai Symposium on Plasma Nonlinear Phenomena, Tohoku University, Sendai, Japan (1984).

14. C. F. Driscoll, K. S. Fine and J. H. Malmberg, "Reduction of Radial Losses in a Pure Electron Plasma," submitted to Phys. Fluids.

15. M. H. Douglas and T. M. O'Neil, "Transport of a Nonneutral Electron Plasma due to Electron Collisions with Neutral Atoms," Phys. Fluids **21**, 920 (1978).

16. D. L. Eggleston, T. M. O'Neil and J. H. Malmberg, "Collective Enhancement of Radial Transport," Phys. Rev. Lett. **53**, 982 (1984).

17. T. M. O'Neil, "Cooling of a Pure Electron Plasma by Cyclotron Radiation," Phys. Fluids **23**, 725 (1980).

18. W. D. White, J. H. Malmberg and C. F. Driscoll, "Resistive Wall Destabilization of Diocotron Waves," Phys. Rev. Lett. **49**, 1822 (1982); W. D. White and J. H. Malmberg, "Feedback Damping of the $l=1$ Dioctron Wave," Bull. APS **27**, 1031 (1982).

19. T. M. O'Neil and C. F. Driscoll, "Transport to Thermal Equilibrium of a Pure Electron Plasma," Phys. Fluids **22**, 266 (1979).

20. S. A. Prasad and T. M. O'Neil, "Finite Length Thermal Equilibria of a Pure Electron Plasma Column," Phys. Fluids **22**, 278 (1979).

2G

21. T. M. O'Neil, "A New Theory of Transport due to Like Particle Collisions," Phys. Rev. Lett. **55**, 943 (1985).

22. C. F. Driscoll, K. S. Fine and J. H. Malmberg, "Transport to Thermal Equilibrium in Pure Electron Plasmas," Bull. APS **30**, 1552 (1985).

23. C. M. Surko *et al*, in *Positrons and Solids, Surfaces and Atoms*, K. F. Canter, ed. (World Scientific, 1986).

24. W. Kells, "Remote Antiproton Sources," IEEE Trans. Nucl. Sci. **NS32**, 1770 (1985).

25. T. M. O'Neil, "Centrifugal Separation of a Multispecies Pure Ion Plasma," Phys. Fluids **24**, 1447 (1981).